JOURNAL OF GEOPHYSICAL RESEARCH, VOL. 114, A07104, doi:10.1029/2009JA014299, 2009

A homogeneous database of sunspot areas covering more than 130 years

L. A. Balmaceda,[1,2] S. K. Solanki,[1] N. A. Krivova,[1] and S. Foster[3]

Received 26 March 2009; accepted 4 May 2009; published 18 July 2009.

[1] The historical record of sunspot areas is a valuable and widely used proxy of solar activity and variability. The Royal Greenwich Observatory regularly measured this and other parameters between 1874 and 1976. After that time records from a number of different observatories are available. These, however, show systematic differences and often have significant gaps. Our goal is to obtain a uniform and complete sunspot area time series by combining different data sets. A homogeneous composite of sunspot areas is essential for different applications in solar physics, among others for irradiance reconstructions. Data recorded simultaneously at different observatories are statistically compared in order to determine the intercalibration factors. Using these data we compile a complete and cross-calibrated time series. The Greenwich data set is used as a basis until 1976, the Russian data (a compilation of observations made at stations in the former USSR) are used between 1977 and 1985, and data compiled by the USAF network are used since 1986. Other data sets (Rome, Yunnan, and Catania) are used to fill up the remaining gaps. Using the final sunspot areas record the Photometric Sunspot Index is calculated. We also show that the use of uncalibrated sunspot areas data sets can seriously affect the estimate of irradiance variations. Our analysis implies that there is no basis for the claim that UV irradiance variations have a much smaller influence on climate than total solar irradiance variations.

Citation: Balmaceda, L. A., S. K. Solanki, N. A. Krivova, and S. Foster (2009), A homogeneous database of sunspot areas covering more than 130 years, *J. Geophys. Res.*, *114*, A07104, doi:10.1029/2009JA014299.

1. Introduction

[2] The total area of all sunspots visible on the solar hemisphere is one of the fundamental indicators of solar magnetic activity. Measured since 1874, it provides a proxy of solar activity over more than 130 years that is regularly used, e.g., to study the solar cycle or to reconstruct total and spectral irradiance at earlier times [e.g., *Brandt et al.*, 1994; *Solanki and Fligge*, 1998; *Li*, 1999; *Li et al.*, 2005; *Preminger and Walton*, 2005; *Krivova et al.*, 2007]. Consequently, a reliable and complete time series of sunspot areas is essential. Since no single observatory made such records over this whole interval of time, different data sets must be combined after an appropriate intercalibration. In this sense, several comparative studies have been carried out in order to get an appropriately cross-calibrated sunspot area data set [see, e.g., *Hoyt et al.*, 1983; *Sivaraman et al.*, 1993; *Fligge and Solanki*, 1997; *Baranyi et al.*, 2001; *Foster*, 2004, and references therein]. They pointed out that differences between data sets can arise because of random errors introduced by the personal bias of the observer, limited seeing conditions at the observation site, different amounts of scattered light, or the difference in the time when the observations were made. Systematic errors also account for a disparity in the area measurements. They are related to the observing and measurement techniques and different data reduction methods. For example, areas measured from sunspot drawings are on average smaller than the ones measured from photographic plates [*Baranyi et al.*, 2001].

[3] In this work, we compare data from Russian stations and the USAF (US Air Force) network as well as from other sources (Rome, Yunnan, Catania) with Royal Greenwich Observatory (RGO) data. This combination provides a good set of observations almost free of gaps after 1976. Combining them appropriately improves the sunspot area time series available at present.

[4] In section 2 we describe the data provided by the different observatories analyzed here. The method to calculate the appropriate cross-calibration factors is explained in section 3.1. The results of the different comparisons are presented in section 4. In section 5 we discuss one central application of sunspot areas: solar irradiance reconstructions. When sunspots pass across the solar disc, a noticeable decrease in the measured total solar irradiance is observed. This effect can be quantified by the photometric sunspot index [*Willson et al.*, 1980; *Foukal*, 1981; *Hudson et al.*, 1982]. This index depends on the positions of the sunspots

[1] Max-Planck-Institut für Sonnensystemforschung, Katlenburg-Lindau, Germany.
[2] Now at GACE, IPL, Universidad de Valencia, Valencia, Spain.
[3] Space and Atmospheric Physics Group, Blackett Laboratory, Imperial College London, London, UK.

0148-0227/09/2009JA014299$09.00

Table 1. Data Provided by the Different Observatories

Observatory	Observation Period	Observing Technique	Coverage (%)	Minimum Area Reported (ppm of Solar Hemisphere)
RGO	1874–1976	photographic plates	98	1
Russia	1968–1991	photographic plates	96	1
SOON	1981–2008	drawings	98	10
Rome	1958–1999	photographic plates	50	2
Catania	1978–1987	drawings	81	3
Yunnan	1981–1992	photographic plates	81	2

on the visible solar disc and on the fraction of the disc covered by the spots, i.e., on the sunspot area. It is thus clear that appropriately cross-calibrated sunspot areas are required for accurate reconstructions of solar irradiance [see *Fröhlich et al.*, 1994; *Fligge and Solanki*, 1997]. We compare results when raw and calibrated data are used to calculate this index and total solar irradiance in section 6. Finally, section 7 presents the summary and conclusions.

2. Observational Data

[5] Data from RGO provide the longest and most complete record of sunspot areas. The data were recorded at a small network of observatories (Cape of Good Hope, Kodaikanal and Mauritius) between 1874 and 1976, thus covering nine solar cycles. Heliographic positions and distance from the central meridian of sunspot groups are also available.

[6] The second data set is completely independent and was published by the *Solnechniye Danniye* (Solar Data) Bulletin issued by the Pulkovo Astronomical Observatory. The data were obtained at stations belonging to the former USSR. These stations provided sunspot areas corrected for foreshortening, together with the heliographic position (latitude, longitude) and distance from center of solar disc in disc radii for each sunspot group. We will refer to this data set as Russian data.

[7] After RGO ceased its programme, the US Air Force (USAF) started compiling data from its own Solar Optical Observing Network (SOON). This network consists of solar observatories located in such a way that 24-h synoptic solar monitoring can be maintained. The basic observatories are Boulder and the members of the network of the US Air Force (Holloman, Learmonth, Palehua, Ramey and San Vito). Also, data from Mount Wilson Observatory are included. This programme has continued through to the present with the help of the US National Oceanic and Atmospheric Administration (NOAA). This data set is referred to by different names in the literature, e.g., SOON, USAF, USAF/NOAA, USAF/Mount Wilson. In the following, we will refer to it as SOON.

[8] Usually multiple measurements are provided for a given sunspot group n on a particular day d coming from different SOON stations, up to a maximum of 6 if all the stations provided information. Normally, at least three values are listed. In order to get a unique value for this group, we calculate averages of sunspot areas recorded on this day d ($A_{n,d}$), including only those values which fulfill the following condition:

$$\overline{A_{n,d}} - 2 \cdot \sigma_A \leq A_{n,d} \leq \overline{A_{n,d}} + 2 \cdot \sigma_A.$$

Here, $\overline{A_{n,d}}$ is the mean value of all the areas measured for the group n on the day d, and σ_A is their standard deviation. The value of σ_A varies from group to group, depending on their sizes and on the time of the solar cycle. Note that, by using this condition we intend to exclude outliers, i.e., those areas whose values differ greatly from the mean for each group. In those cases where the number of stations providing data is 1, the area for that group is taken from this single source. If the number is 2, the area for that group is the mean of the areas measured by both stations.

[9] After that, sunspot areas for individual groups are summed up to get the daily value. Also averaged are latitudes and longitudes of each sunspot group recorded by those observatories whose data are employed to get the mean sunspot area.

[10] These three data sets (RGO, Russia and SOON) are the prime sources of data that we consider, since they are the most complete, being based on observations provided by multiple stations. A number of further observatories have also regularly measured sunspot areas during the past decades. The record from Rome Astronomical Observatory, whose measurements began in 1958, covers more than three consecutive and complete solar cycles. It has several years of observations in common with Russian stations and SOON as well as with RGO. This is perhaps the only source of data with a long period of overlap with all three prime data sets. The database from Rome is used to compare the results obtained from the other observatories and also to fill up gaps whenever possible. Unfortunately, its coverage is limited by weather conditions and instrumentation problems. Whenever available, data from Yunnan Observatory in China and Catania Astrophysical Observatory in Italy are also used to fill up the remaining gaps. In Catania, daily drawings of sunspot groups were made at the Cooke refractor on a 24.5 cm diameter projected image from the Sun, while the measurements provided by the Chinese observatory are based on good quality white light photographs. Table 1 summarizes the information provided by each observatory: the period in which observations were carried out, the observing technique, the coverage (i.e., the percentage of days on which measurements were made) and the minimum area reported by each observatory. Areas corrected for foreshortening are provided in all the cases. Directly observed or projected areas, can be derived using the heliographic positions for sunspot groups and hence heliocentric angle, θ, or μ values ($\cos\theta$). Striking is the relatively large minimum area considered by the SOON network. This suggests that many smaller sunspots are neglected in this record.

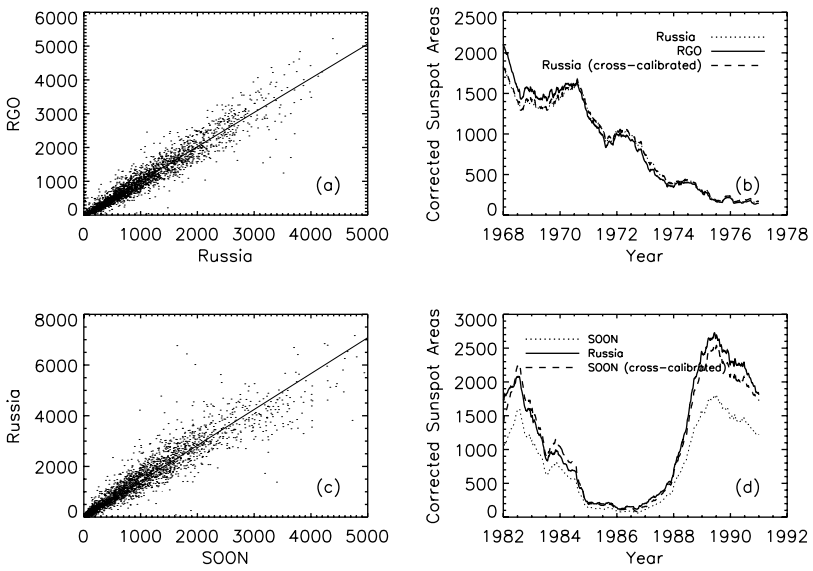

Figure 1. Comparison of sunspot areas corrected for foreshortening obtained by different observatories. (a and b) RGO versus Russia and (c and d) Russia versus SOON. Figures 1a and 1c show scatterplots. Solid lines represent linear regressions to the data neglecting a possible offset (i.e., forced to pass through zero) as well as data points close to the origin and the outliers lying outside the $\pm 3\sigma$ interval from the fit. Figures 1b and 1d show 12-month running means of sunspot areas versus time. Solid curves show the data used as basis level, dotted curves are the data from the second observatory, and dashed curves are the calibrated areas.

[11] All the data used in this work were extracted from the following Web site: http://www.ngdc.noaa.gov/stp/SOLAR/ftpsunspotregions.html.

3. Analysis

3.1. Cross-Calibration Factors

[12] Daily sunspot areas from two different observatories are directly compared on each day on which both had recorded data. We deduced multiplication factors needed to bring all data sets to a common scale, namely that of RGO, which is employed as fiducial data set.

[13] For this, the spot areas from one data set are plotted versus the other (see Figures 1a and 1c). The slope of a linear regression forced to pass through the origin (see Appendix A) can be used to calibrate the sunspot area record considered auxiliary, A^{aux}, to the areas of another basic data set, A^{bas}:

$$A^{bas} = b \cdot A^{aux}. \tag{1}$$

[14] First, this analysis is applied to all the points. The slope thus obtained is taken to be the initial estimate for a second analysis where not all the points are taken into account. Outliers are excluded by taking only points within $3\sigma_{fit}$ from the first fit, where $\sigma_{fit} = \sqrt{\frac{1}{N-1}\sum_{i=1}^{N}\left(A_i^{bas} - b \cdot A_i^{aux}\right)^2}$. Also, only areas lying above the line joining the points (0, $3\sigma_{fit}$) and ($3\sigma_{fit}$, 0) are considered. Through this measure points close to the origin are excluded since they introduce a bias.

[15] Ordinary least-square regression cannot be applied in this case, for the following reasons: (1) the distinction between independent and dependent variables is arbitrary, (2) the data do not provide formal errors for the measurements, and (3) the intrinsic scatter of the data may dominate any errors arising from the measurement procedure of sunspot areas. A method that treats the variables symmetrically should be used instead.

[16] To this purpose, the same procedure is repeated after interchanging the data sets taken as a basis and as auxiliary. For the reasons outlined in Appendix A, the inverse value of the slope now obtained, b', differs from the slope b obtained in the first place. Therefore, the final calibration factor is then calculated by averaging these two values: b and $1/b'$. This method is referred to as "bisector line" [*Isobe et al.*, 1990].

[17] An alternative method to find the calibration factors is described in Appendix B. This second method does not neglect the sunspot areas close to zero. In contrast, it gives equal weight to all values. The calibration factors obtained in this way are thus less accurate during high activity levels, when solar irradiance is most variable. Since the reconstruction of solar irradiance is a key application of the new cross-calibrated sunspot area record, we select the method described above rather than the one presented in Appendix B. Of course, for other applications, this method may happen to be more appropriate. Therefore, in Table 3 we also give the factors obtained in this way. The difference between the factors obtained by the 2 methods is generally less than 5%, although differences as large as 12% can be reached for factors deduced from corrected sunspot areas.

[18] Data series that do not overlap in time can be intercalibrated using the Zurich sunspot number as a common index [*Fligge and Solanki*, 1997; *Vaquero et al.*, 2004]. Since this approach requires an additional assumption, namely that the size distribution of sunspots [*Bogdan et al.*, 1988; *Baumann and Solanki*, 2005] remains unchanged over time we avoid using it for calibration purposes [*Solanki and Unruh*, 2004]. We use this comparison only for confirmation

Table 2. Calibration Factors for the Different Observatories

Observatory 1	Observatory 2	Overlap Period	Calibration Factor PA	Calibration Factor CA	Correlation Coefficient PA	Correlation Coefficient CA
RGO	Russia	1968–1976	1.019 ± 0.067	1.028 ± 0.083	0.974	0.961
Russia	SOON	1982–1991	1.402 ± 0.131	1.448 ± 0.148	0.953	0.942
RGO	Rome	1958–1976	1.095 ± 0.086	1.097 ± 0.084	0.969	0.963
Russia	Rome	1968–1990	1.169 ± 0.058	1.227 ± 0.107	0.947	0.907
SOON	Rome	1982–1999	0.791 ± 0.105	0.846 ± 0.138	0.946	0.902
Russia	Yunnan	1968–1990	1.321 ± 0.215	1.365 ± 0.242	0.959	0.947
SOON	Yunnan	1982–1992	0.913 ± 0.113	0.907 ± 0.131	0.948	0.955
Russia	Catania	1978–1987	1.236 ± 0.052	1.226 ± 0.059	0.959	0.909
SOON	Catania	1982–1987	0.948 ± 0.042	0.925 ± 0.097	0.967	0.949
RGO	SOON	via Russia	1.429 ± 0.163	1.489 ± 0.194	-	-
RGO	Catania	via Russia	1.240 ± 0.099	1.234 ± 0.119	-	-
RGO	Yunnan	via Russia	1.346 ± 0.237	1.403 ± 0.273	-	-

of the results obtained from the direct measurements, so that the new record is completely independent of the sunspot number time series.

3.2. Error Estimates

[19] A single calibration factor is calculated for the whole period of overlap between data sets obtained by two observatories. This is repeated once for the projected areas and those corrected for foreshortening provided by the different observatories.

[20] In some cases, however, the relation between two data sets was found to evolve with time. This can be seen in Figures 1b and 1d, in which the 12-month running means of sunspot area records are plotted versus time. Both Figures 1b and 1d show that even after cross calibration the two data sets do not run in parallel but rather have systematic relative offsets over particular periods of time (lasting multiple years). Therefore factors for different subintervals are also calculated, in order to estimate the uncertainties of the final factors. This is performed by separating different solar cycles. When the whole interval of overlap does not cover more than one cycle, then the division is made when a change in the behavior is observed. See, e.g., the comparison between RGO and Russian data in Figure 1b, where the change takes place after year 1971. Before that year, Russian areas are on average smaller than those from RGO, while the situation is reversed afterward. The uncertainty in the final factors is thus the combination of the uncertainties due to the cycle-to-cycle variations (different factors for different cycles and/or subintervals), σ_{cyc}, the difference between b and b', σ_{dif}, and the errors, σ_{slope}, in determining the slopes so that: $\sigma = \sqrt{\sigma_{cyc}^2 + \sigma_{dif}^2 + \sigma_{slope}^2}$. The main source of uncertainties being the fact that the relationship between two given observatories during the period they overlap is not uniform. Therefore, the smallest errors are obtained when this period is short (see, e.g., Russia – Catania, SOON – Catania in Table 2). On the other hand, the largest errors are found in the comparison between Russia and Yunnan. This is discussed in more detail in section 4.

4. Results and Discussion

4.1. Comparison Between Sunspot Areas

[21] The results of the analysis described in section 3 are summarized in Table 2. The first two columns give the names of the data sets being compared. The observatories whose data are taken as the basis are indicated as observatory 1, while the observatories whose data are recalibrated are indicated as observatory 2. The third column shows the interval of time over which they overlap. In the next two columns we list the calibration factors by which the data of observatory 2 have to be multiplied in order to match those of observatory 1. The factors for the originally measured areas (projected areas, PA) and for the areas corrected for foreshortening (CA) are given, in columns 5 and 6, respectively. The two last columns list the corresponding correlation coefficients between the two data sets.

[22] With one exception the correlation coefficients for the projected areas are larger than for the ones corrected for foreshortening. This is not unexpected, since errors in the measured position of a sunspot increase the scatter in the areas corrected for foreshortening, while leaving the projected areas unaffected.

[23] In the following we discuss the results in greater detail. The overlap between RGO and Russian data covers the descending phase of cycle 21. As can be seen from Figures 1a and 1b the two sets agree rather well with each other. The cross-calibration factor is very close to unity, although the difference between the two data sets displays a trend with time. Before 1971, areas from RGO are larger (6% for projected, 8% in case of corrected for foreshortening) than Russian measurements, whereas after that time areas from the Russian data set are 8% larger (see Figure 1b) for both, projected and corrected areas. This trend remains also after recalibrating the Russian data, because a single factor is not sufficient to remove this effect. Since it is not clear which (or both) of these two data sets contains an artificial drift, we do not try to correct for it.

[24] Russian and SOON areas display more significant differences (see Figures 1c and 1d). The overlap covers the period from 1982 to 1991, or cycles 21 and 22. During the whole time interval, SOON areas appear to be smaller (by on average 40% for projected and 45% for the corrected ones) than those of the Russian data. This is mainly due to the significant difference in the minimum value of the counted sunspots (1 ppm of the solar hemisphere for Russian versus 10 ppm of the solar hemisphere for SOON observations, see Table 1). As can be seen from Figure 1d, data from these two records also do not run in parallel, exhibiting quite a significant trend relative to each other (compare solid and dashed curves).

[25] In general, it was found that areas measured by the SOON network as well as those by the Rome, Catania and

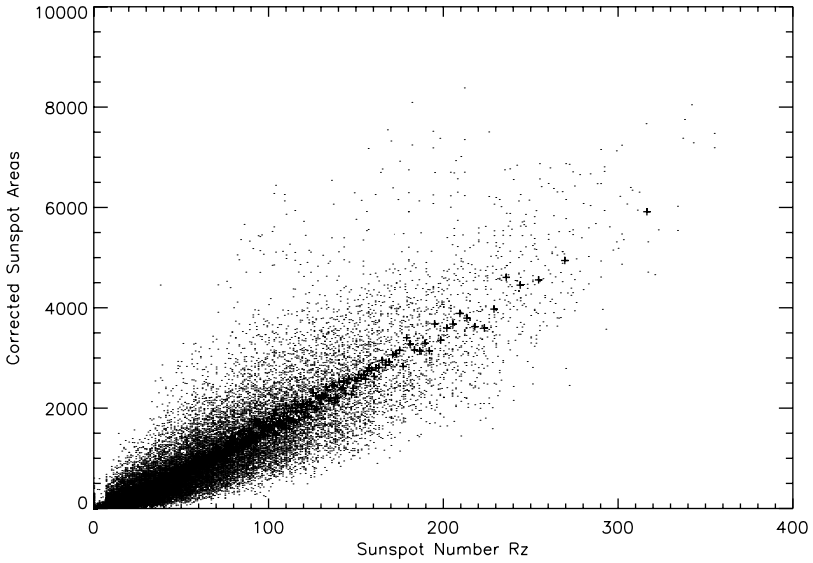

Figure 2. Sunspot areas corrected for foreshortening versus sunspot number, R_z, for measurements made by RGO. The dots represent daily values between 1874 and 1976. Each plus symbol represents an average over bins of 50 points.

Yunnan observatories are on average smaller than areas reported by RGO and Russian stations, which agrees with the fact that the minimum areas of individual spots included into these two records are the smallest. For the same reason, SOON areas are smaller on average than the measurements from other data sets: the minimum area of the recorded spots is a factor of 3 to 10 higher for SOON than for the other observatories.

[26] The last three lines of Table 2 give the factors by which SOON, Catania and Yunnan data need to be multiplied in order to match the RGO data. Since none of these data sets overlap with RGO we have used the Russian data as intermediary. Of course, correlation coefficients cannot be determined in this case. The factor needed to calibrate SOON data to the RGO data set is 1.43 for projected areas, in good agreement with the results by *Hathaway et al.* [2002] and *Foster* [2004], who both give 1.4. In the case of areas corrected for foreshortening the factor found here is ~7% larger, being 1.49.

4.2. Comparison With Sunspot Number

[27] The relationship between the Zurich relative sunspot number, R_z, and sunspot area (from a single record) shows a roughly linear trend with a large scatter. In Figure 2 we plot sunspot areas corrected for foreshortening, A_S, for RGO measurements versus R_z. We have chosen A_S from RGO since this is the longest running data set. The plus signs represent data points binned in groups of 50. These points indicate that the relationship is roughly, but not exactly linear. In particular at low R_z values, A_S appears to be too small, possibly because of the cutoff in the A_S measurements. However, this behavior may reflect also the particular definition of $R_z = k(10g + s)$, where g is the number of sunspot groups, s the total number of distinct spots and k the scaling factor (usually <1) which depends on the observer and is introduced in order to keep the original scale by Wolf [*Waldmeier*, 1961]. In this definition, even a small group of sunspots is given a nearly equally large weight as a large group. It is observed from this plot that a given value of R_z corresponds to a range of values of sunspot areas. However, the scatter due to points within a single cycle is larger than the scatter from cycle to cycle.

[28] When studying the relationship between A_S and R_z for individual cycles, it was observed that in some cases the scatter is significantly higher. In such cycles, large areas are observed while R_z remains low. In particular, the shape of A_S cycles resembles that of R_z cycles, but individual peaks are more accentuated in A_S. This could be also a consequence of the definition of R_z, regarding the large weight given to the groups. *Fligge and Solanki* [1997] already showed that, in general, the relationship between A_S and R_z changes only slightly from one cycle to the next, with the difference being around 10%.

[29] Figure 3 shows the comparison between RGO and SOON sunspot areas corrected for foreshortening with the sunspot number. We have binned the data from each observatory every 50 points according to the sunspot number. The uncalibrated areas from SOON lie significantly below the ones from RGO. After multiplying SOON data by the calibration factor of 1.49 found in section 4.1, they display practically the same relationship to R_z as the RGO data.

4.3. Cross-Calibrated Sunspot Area Records

[30] In a next step we create records of projected and corrected sunspot areas covering the period from 1874 to 2008 that are consistently cross-calibrated to the RGO values. We use RGO, Russia and SOON measurements as the primary sources of data. As shown by Table 1, these sources provide the sets of sunspot area measurements, with the least number of gaps.

[31] The individual periods of time over which each of these is taken as the primary source are as follows: 1874–1976 (RGO), 1977–1986 (Russia), and 1987–2008 (SOON). The final sunspot area composite is plotted in Figure 4 (solid curve), and is tabulated in Data Set S1

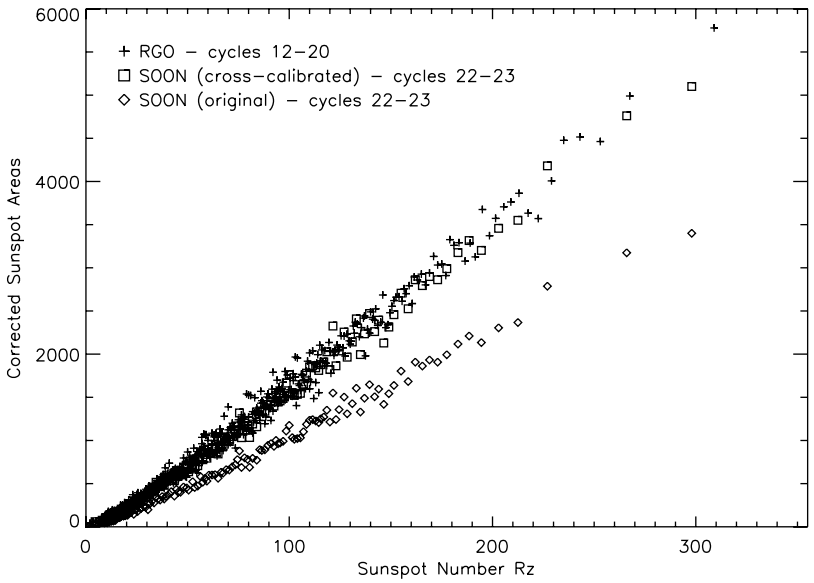

Figure 3. Sunspot areas corrected for foreshortening versus Zurich relative sunspot number, R_z, for measurements made by RGO and SOON. Each symbol represents an average over bins of 50 points. The original data from SOON are represented by diamonds, and those after multiplication by a calibration factor of ~1.5 in order to match RGO data are represented by squares.

(see auxiliary material).[1] We have chosen to use the Russian data set until 1986 for the simple reason that this year corresponds to the solar minimum. In this way, each data set describes different solar cycles (see Figure 4). We are aware that this is only approximately correct since sunspots from consecutive cycles overlap during a short period of time, but this is a second-order effect. In this combination we opt to multiply the post-RGO measurements by the factors obtained here since RGO areas data set is by far the longest running and relatively homogeneous source. Any data gaps in the primary source are filled using data from one of the other two primary records (if available), or data from Rome and Yunnan, properly recalibrated. The two last-named series allowed us to fill up the gaps over a total of 115 days. In this way, gaps in the final composite cover only ~8% of the total length of the combined data set of 49308 days.

5. Photometric Sunspot Index

[32] The passage of sunspots across the solar disc causes a decrease in the total solar irradiance. This effect can be quantified by estimating the photometric sunspot index, P_S [*Hudson et al.*, 1982]. First, the deficit of radiative flux, ΔS_S, due to the presence of a sunspot of area A_S is calculated as:

$$\frac{\Delta S_S}{S_Q} = \frac{\mu A_S (C_S - 1)(3\mu + 2)}{2}. \quad (2)$$

This value is expressed in units of S_Q, the solar irradiance for the quiet Sun (i.e., solar surface free of magnetic fields). S_Q = 1365.5 W/m^2 is taken from the PMOD composite of measured solar irradiance [*Fröhlich*, 2003, 2006]. We use the areas composite obtained here, A_S, and the heliocentric positions, μ, of the sunspots present on the solar disc. The residual intensity contrast of the sunspot relative to that of the background photosphere $C_S - 1$ is taken from *Brandt et al.* [1992]. It takes into account the dependence of the sunspot residual intensity contrast on sunspot area; that is, larger sunspots are darker than smaller spots, as has recently been confirmed on the basis of MDI data by *Mathew et al.* [2007]. Following *Brandt et al.* [1992, 1994] and *Fröhlich et al.* [1994] we use:

$$C_S - 1 = 0.2231 + 0.0244 \cdot \log(A_S). \quad (3)$$

[33] Finally, summing the effects from all the sunspots present on the disc we obtain:

$$P_S = \sum_{i=1}^{n} \left(\frac{\Delta S_s}{S_Q} \right)_i. \quad (4)$$

Figure 5 shows the 12-month running mean time series of the P_S index for the period 1874–2008. The daily P_S values are also listed in Data Set S1 (see auxiliary material).

6. An Example of Errors Introduced by an Uncritical Use of Uncalibrated Sunspot Areas Data Sets

[34] Variations of solar irradiance on time scales longer than approximately a day are caused by the passage of dark sunspots and bright faculae across the solar disc. Because of the different wavelength dependences of their contrasts, the contribution of faculae is higher in the UV than in the visible or IR, whereas the contribution of sunspots dominates increasingly with increasing wavelength [*Solanki and*

[1] Auxiliary materials are available at ftp://ftp.agu.org/apend/ja/2009ja014299.

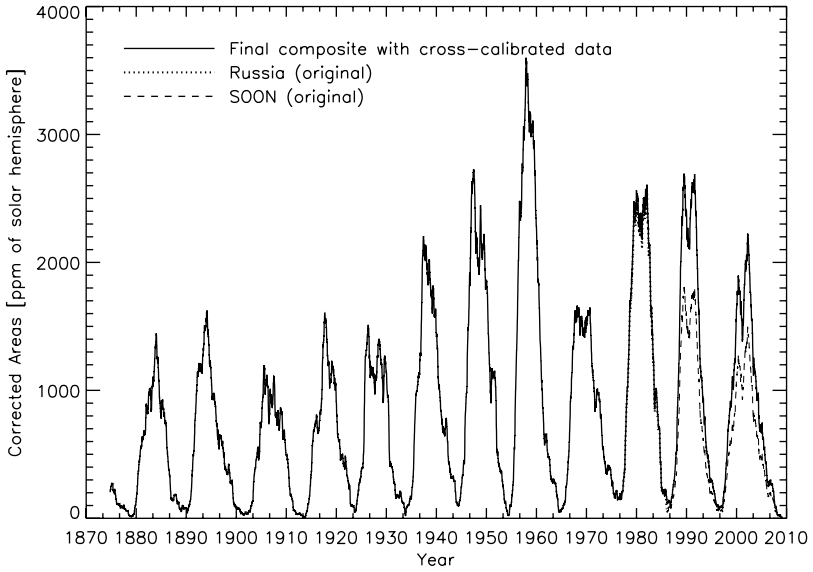

Figure 4. Twelve-month running means of sunspot areas corrected for foreshortening of the final composite using the factors given in Table 2 (solid curve). Also plotted are the Russian and SOON data entering the composite prior to calibration.

Unruh, 1998; *Unruh et al.*, 1999]. Thus employment of a faulty or inconsistent sunspot or faculae time series to reconstruct solar total and UV irradiance can lead to systematic differences between them.

[35] Now, it has been claimed that variations of solar UV irradiance are less important for climate than variations of solar total irradiance, S [*Foukal*, 2002; *Foukal et al.*, 2006]. These results are based on uncalibrated sunspot areas including both the Greenwich and the SOON data sets. Here we show that when sunspot areas after appropriate intercalibration as described in section 3.1 are employed, total and UV solar irradiance behave similarly.

[36] We redo the analysis of *Foukal* [2002], but employing the cross-calibrated time series of sunspot areas obtained here. For the facular contribution we employ the same proxy as *Foukal* [2002], a monthly mean time series of plage plus enhanced network areas, A_{PN}. This data set was kindly provided by P. Foukal. Areas were measured from spectroheliograms and photoheliograms in the K line of Ca II obtained at Mount Wilson, McMath-Hulbert and Big Bear observatories in the period 1915–1984 [*Foukal*, 1996, 1998]. Later, this time series was extended until 1999 using data from Sacramento Peak Observatory (SPO). The data cover the period August 1915 to December 1999 inclusive. The identification of plages and enhanced network was performed by several observers. Details about the reduction procedure to derive the A_{PN} index are given by *Foukal* [1996]. A_{PN} values are expressed in fractions of the solar disc.

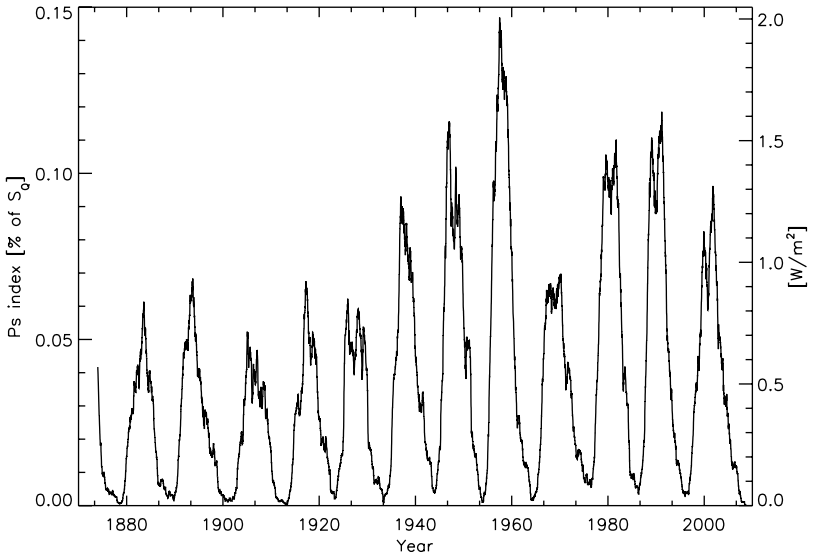

Figure 5. Twelve-month running mean of the photometric sunspot index, P_S, computed using the sunspot areas composite produced here. The y axis is expressed in percent of S_Q, the irradiance of the quiet Sun.

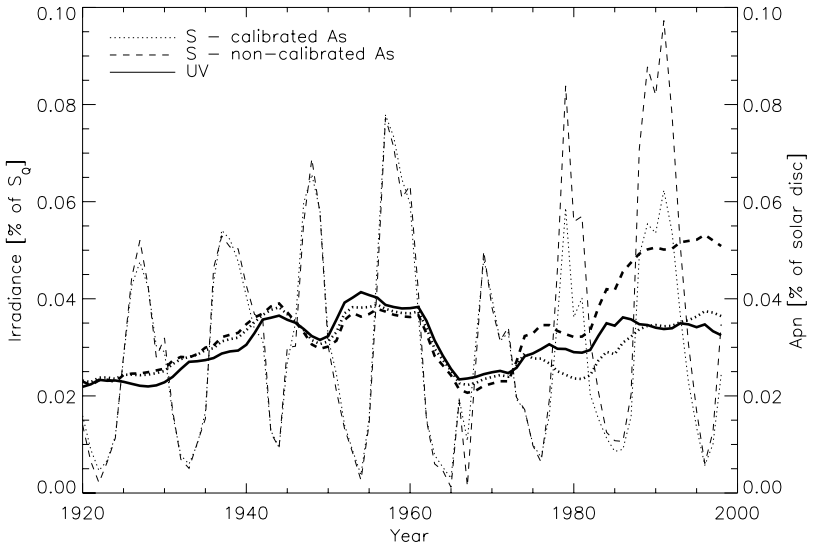

Figure 6. Eleven-year running mean of total solar irradiance based on calibrated areas (dotted line), noncalibrated areas (dashed line), and UV irradiance given by the variations in the A_{PN} (solid line). The thin lines represent 1-year means of solar irradiance based on calibrated areas (dotted line) and noncalibrated areas (dashed line). The y axis is expressed in percent of S_Q, the irradiance of the quiet Sun.

[37] Total and UV solar irradiance time series are reconstructed following *Foukal* [2002]. According to that approach, enhancements in total solar irradiance are proportional to the difference in plage, A_{PN}, and sunspot areas, A_S, whereas enhancements in UV irradiance are proportional to the plage areas alone. As a first step, residuals of solar irradiance after removing the sunspot darkening, $S - P_S$, are calculated for the time when irradiance measurements are available, i.e., from 1978 till present. This quantity, $S - P_S$, is a measure of facular contribution to the total irradiance. Total solar irradiance measurements, S, are taken from the PMOD composite derived from different instruments with best allowance for their degradation and intercalibration [*Fröhlich*, 2000, 2006]. Then, a regression relation of the form: $S - P_S = b \cdot A_{PN} + a$ is constructed between the monthly mean values of these residuals and of the plage areas, A_{PN}. This regression relation is then used to reconstruct the residuals $(S - P_S)_{rec}$ between 1915 and 1999 when values of A_{PN} are available. The reconstructed total solar irradiance is finally obtained by just adding back the time series of P_S over this period.

[38] Figure 6 shows the 11-year running means of the reconstructed total irradiance using calibrated (thick dotted line) and noncalibrated (thick dashed line) data. The thin lines represent the 1-year means of both reconstructions. The curves were scaled in order to highlight the difference in the upward trend after 1970. The dashed curve represents the UV irradiance, i.e., the solar flux at wavelengths shorter than 250 nm. Its variability is determined mainly by the bright magnetic plages in active regions and enhanced network produced as these regions decay. Its reconstruction follows the same steps as of the total solar irradiance, except that the last step (adding back the P_S) is not carried out.

[39] The total irradiance reconstructed by *Foukal* [2002], which is very similar to the dashed curve in Figure 6, shows a clear upward trend after the year 1976 due to the strong presence of faculae that is not balanced by increased sunspot area. The UV irradiance does not display such a prominent rise, however. This result was interpreted by *Foukal* [2002] as evidence for a strongly different behavior of the total irradiance and UV irradiance and consequently their very different influence on the Earth's climate. In particular, the fact that the TSI correlates much better with global climate than the UV irradiance during the last three decades led *Foukal* [2002] to propose that UV irradiance influences global climate less than total irradiance. However, we find here that this behavior is no longer observed when appropriately calibrated areas are used. The shape of the total irradiance estimated from calibrated data now follows closely the shape of the variation in A_{PN}, i.e., the UV irradiance [cf. *Solanki and Krivova*, 2003]. It is not by chance that the two reconstructions of S start to diverge in $\sim$1976 since at that time the record of A_S from RGO ends.

[40] We stress that the simple approach used here to reconstruct total and UV solar irradiance has shortcomings. One concerns the A_{PN} time series, which is based on uncalibrated spectroheliograms. Film calibration in photographic plates and variable image quality are some of the factors that introduce uncertainties in the extraction of the features and need to be taken into account. They affect the correct identification of different features in the CaII K images which is based on criteria of decreasing intensity, decreasing size or decreasing filling factors [*Worden et al.*, 1998]. Another concerns the simplicity of the model assumed here, which successfully reproduces the cyclic variation but does not contain a secular trend, unlike more detailed and complete recently developed models, for instance, *Foster* [2004], *Wang et al.* [2005], and *Krivova et al.* [2007]. Such a secular trend can be produced by long-term changes in the network, which is only poorly sampled by the A_{PN} data employed here. These shortcomings have no influence on the drawn conclusions, however. It is not the aim of this section to produce realistic records of total and UV irradiance, but rather to demonstrate the importance of using a carefully cross-calibrated sunspot areas time series. In particular, our conclusion that total solar irradiance shows

no strong upward trend in three decades since 1976 is supported by the irradiance composite of *Fröhlich* [2000, 2006] and the modeling work of *Wenzler et al.* [2006].

7. Summary and Conclusions

[41] In this work, we have compared sunspot areas measured at different observatories. We found a good agreement between sunspot areas measured by Russian stations and RGO, while a comparison of sunspot areas measured by the SOON network with Russian data shows a difference of about 40% for projected areas and 44% in areas corrected for foreshortening. This is at least partly due to the different minimum areas of sunspots taken into account in these data sets: smallest areas included in the RGO and Russian records are 10 times smaller than those in the SOON series (see Table 1). Histograms of sunspot areas show that such small sunspots are rather common [*Bogdan et al.*, 1988; *Baumann and Solanki*, 2005]. SOON sunspot areas are combined with those from RGO and Russia by multiplying them by a factor of 1.43 in the case of projected areas and 1.49 in the case of areas corrected for foreshortening. Data from other observatories are employed to fill up some of the remaining gaps. In this manner, a consistent sunspot area database is produced from 1874 to 2008.

[42] A properly cross-calibrated sunspot areas data set is central for, e.g., reliable reconstructions of total and spectral solar irradiance. In order to demonstrate this, we have also presented a simple reconstruction of total and UV solar irradiance based on sunspot and plages plus enhanced network areas for the period 1915–1999. We showed that the use of data of different sources directly combined, without a proper cross calibration can lead to significantly erroneous estimates of the increase of solar irradiance in the last decades. This means in particular that the claim of *Foukal* [2002] that UV solar irradiance is far less effective in driving climate change than total solar irradiance has no basis.

[43] Data from additional observatories, such as Debrecen Observatory in Hungary [*Győri et al.*, 1998, 2000], will help to improve the sunspot areas record even further. Another interesting possibility not explored here would be the comparison with data from spaceborne observations, which are unaffected by seeing. SOHO/MDI [*Scherrer et al.*, 1995] provides continuous data free of atmospheric effects since 1996 till present. *Győri et al.* [2005] and *Győri and Baranyi* [2006] have presented a comparison between areas measured by Debrecen Observatory and MDI for 1996 and 1997. After applying the same procedure for determining sunspot areas to both data sets, they found that MDI areas are 17% larger. They attribute this difference to the smaller scale of MDI images, with respect to that of Debrecen data. *Wenzler* [2005], on the other hand, compared umbrae and penumbrae areas derived from continuum images taken at the Kitt Peak Observatory (KP) and MDI. From the analysis of 24 selected days at different levels of solar activity between 1997 and 2001, he obtained almost identical values for locations and areas for both data sets by applying an appropriate threshold. He also compared total daily KP sunspot areas and the composite presented here. The comparison showed that SPM areas are about 4% lower for the period 1992–2003 (2055 days). This shows that it is possible to combine ground-based and space-based measurements of sunspot areas into a single time series.

Appendix A: On the Effect of Including Offset in the Calculation of Cross-Calibration Factors

[44] Let us consider sunspot areas recorded by two different observatories, observatory 1 and observatory 2, during the same period. Let b be the slope of the linear regression when the area recorded by observatory 2 is the independent variable and b' the slope when the area recorded by observatory 1 is the independent variable. In the ideal case, $b = 1/b'$. However for real data sets this is not true. There are two reasons for this. Firstly, since sunspot areas cannot be negative, values close to zero introduce a bias into the regression coefficients. As a result, the slopes we obtain including an offset (dashed lines in Figure A1) are typically lower than the ones obtained by considering no offset (solid lines in Figure A1). In particular, the obtained b is always lower than $1/b'$, whereas b' is lower than $1/b$. In order to overcome this, we force the fit to go through the origin (solid lines in Figure A1). The corresponding slopes typically increase, such that values of b and $1/b'$ become closer to each other, although they still differ. Secondly, when carrying out a linear regression to the relationship between the observatories, we assume measurements by one of them to be free of errors, whereas in reality both records are subject to errors. This immediately produces different regressions depending on which data set is plotted on the ordinate. This is well illustrated by comparing the encircled data point in Figures A1a and A1b (it corresponds to the same data point in both). In Figure A1a, the point significantly lowers the regression slope, since there are hardly any data points at that location of the x axis, while in Figure A1b its influence is small, since it now lies at a well populated part of the x axis. By removing such outliers, we further reduce the difference between b and $1/b'$, but they are still not identical for purely statistical reasons. Therefore, as final factors we take the average between b and $1/b'$ [*Isobe et al.*, 1990].

[45] A more complicated case is the one when there is a significant offset between observatory 1 and observatory 2, for example due to the difference in the minimum area of the considered spots (see, e.g., Figure A1c and Table 1). In this case it may happen that b is not lower than $1/b'$. Then the slopes obtained by forcing the fit to go through zero do not necessarily improve the original ones. However, we apply the same procedure, neglecting the offset, for the following reasons: (1) the magnitude of the offset is rather uncertain because of the bias introduced by the positivity of the sunspot areas; (2) in doing this we may introduce some errors mainly at low values of sunspot areas, whereas values obtained during high activity levels which are of higher priority here are on average relatively reliable; (3) the real slope still lies in the range $[b, 1/b']$ (or $[b', 1/b]$) so that an average of b and $1/b'$ (or b' and $1/b$) is a good approximation and, finally, (4) there are only few such cases (like the comparisons between areas from Russia and Rome and from Rome and SOON shown in Figure A1).

[46] An additional possible reason for the difference between b and $1/b$' may be that the true relationship is

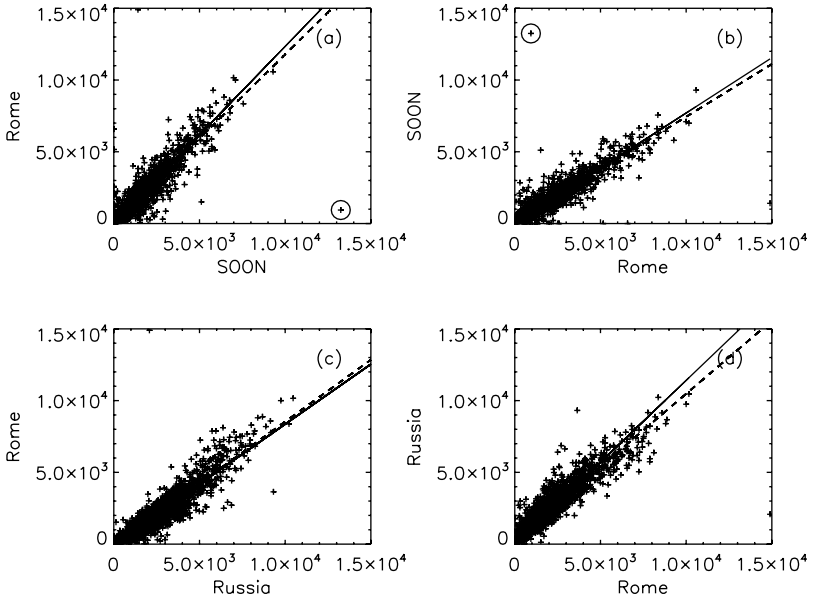

Figure A1. Comparison between sunspot areas recorded by different observatories. Areas are in units of millionths of the solar disc. The lines represent linear regressions to the data: standard (dashed) and forced to pass through the origin (solid). The encircled data point is discussed in the text.

nonlinear. However, the scatter in the data is too large to reach any firm conclusion on this.

Appendix B: An Alternative Method to Calculate Cross-Calibration Factors

[47] In addition to the method described in section 3.1 and Appendix A to cross calibrate different sunspot area data sets, we also performed the cross calibration by varying a parameter f (defined below) in order to minimize a merit function $\mathcal{M}$, calculated over the N days on which both A^{bas} and A^{aux} are available:

$$\mathcal{M} = \sum_{i=1}^{N} \left[A_{t_i}^{bas} - f \cdot A_{t_i}^{aux} \right]^2. \tag{B1}$$

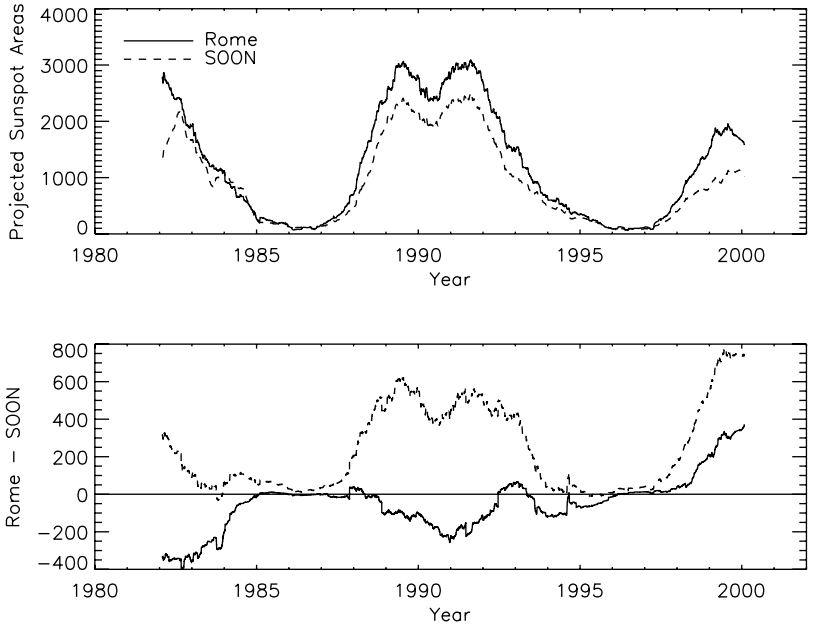

Figure B1. (top) Twelve-month running means of projected sunspot areas. Areas are in units of millionths of the solar disc. They correspond to original values without any calibration. The solid line represents data from the Rome Observatory, and the dashed line represents data from SOON. (bottom) The solid line represents the 12-month running mean of the difference between data from these two observatories after calibrating the data. The dashed line is the difference between the original data from both observatories.

Table 3. Calibration Factors for Projected and Corrected Sunspot Areas Measured by Different Observatories Obtained by Minimizing $\mathcal{M}$[a]

Observatory 1	Observatory 2	Calibration Factor PA	Calibration Factor CA	$\mathcal{M}$ PA	$\mathcal{M}$ CA
RGO	Russia	1.014	1.012	68.9	94.6
Russia	SOON	1.352	1.399	136.1	242.7
RGO	Rome	1.083	1.073	61.3	70.3
Russia	Rome	1.121	1.106	220.5	185.9
SOON	Rome	0.764	0.733	215.8	157.6
Russia	Yunnan	1.279	1.326	111.5	130.6
SOON	Yunnan	0.895	0.882	75.6	87.9
Russia	Catania	1.205	1.197	202.1	164.5
SOON	Catania	0.924	0.853	197.5	244.5

[a]See Appendix B.

[48] The merit function is used here since because of the lack of individual errors for daily measurements the classical definition of χ^2 cannot be applied.

[49] In order to find the absolute minimum of $\mathcal{M}$ irrespective of the presence of any secondary minima, a genetic algorithm called Pikaia is used (http://www.hao.ucar.edu/modeling/pikaia/pikaia.php) [*Charbonneau*, 1995].

[50] In Figure B1 we show the comparison between data from SOON and Rome, which overlap for a long period of time. A 12-month running mean of the original data versus time (Figure B1, top) as well as the difference between the data from the two observatories, for both original and calibrated data (Figure B1, bottom), are shown.

[51] In Table 3, values of the calibration factors for projected sunspot areas and for areas corrected for foreshortening obtained using this technique are listed. The corresponding values for $\mathcal{M}$ are also tabulated. In all cases, these factors are lower than the ones found as explained in section 3.1 and Appendix A. Note, however that if we first form (monthly or yearly) running means of A^{bas} and A^{aux} before minimizing $\mathcal{M}$ we obtain calibration factors much closer to those listed in Table 2. This has got to do with the fact that outliers are given a much smaller weight when forming running means than if taking the squared difference between daily data.

[52] This technique differs from the one discussed in section 3.1 and Appendix A in that here the same weight is given to maximum and minimum phases of solar cycle. It can be seen from Figure B1 that after calibration the difference between both data sets is very close to zero during activity minimum. However, during times of high solar activity this calibration technique does not give as accurate results.

[53] As mentioned before, one of the most important applications of sunspot areas data sets is irradiance reconstruction. So we intend to produce a homogeneous and as complete as possible time series of sunspot areas that can be used in irradiance models to describe adequately the variations. Since sunspot contribution to these variations is most important during times of high activity, a method giving larger weight to periods of high activity (large spot areas) should provide a more appropriate calibration factor. For this reason, we use the factors obtained with the method explained in section 3.1 and Appendix A as the default. Note, however, that in almost all cases factors obtained by the two methods agree within the given uncertainties (even if equation (B1) is applied to daily data, without first forming running means).

[54] **Acknowledgments.** This work was supported by the Deutsche Forschungsgemeinschaft (DFG) project SO 711/1-1. We thank M. Lockwood for his encouragement and critical discussions and P. Foukal for providing the plage and enhanced network areas data set as well for the information and techniques used by him. The authors would also like to thank the anonymous referees for useful comments that contributed to the improvement of the paper.

[55] Amitava Bhattacharjee thanks Philip Judge and another reviewer for their assistance in evaluating this paper.

References

Baranyi, T., L. Gyori, A. Ludmány, and H. E. Coffey (2001), Comparison of sunspot area data bases, *Mon. Not. R. Astron. Soc.*, *323*, 223–230, doi:10.1046/j.1365-8711.2001.04195.x.

Baumann, I., and S. K. Solanki (2005), On the size distribution of sunspot groups in the Greenwich sunspot record 1874–1976, *Astron. Astrophys.*, *443*, 1061–1066, doi:10.1051/0004-6361:20053415.

Bogdan, T. J., P. A. Gilman, I. Lerche, and R. Howard (1988), Distribution of sunspot umbral areas—1917–1982, *Astrophys. J.*, *327*, 451–456, doi:10.1086/166206.

Brandt, P. N., W. Schmidt, and M. Steinegger (1992), Photometry of sunspots observed at Tenerife, in *Solar Electromagnetic Radiation Study for Solar Cycle 22*, edited by R. F. Donnelly, pp. 130–134, Kluwer Acad., Dordrecht, Netherlands.

Brandt, P. N., M. Stix, and H. Weinhardt (1994), Modeling solar irradiance variations with an area dependent photometric sunspot index, *Sol. Phys.*, *152*, 119–124.

Charbonneau, P. (1995), Genetic algorithms in astronomy and astrophysics, *Astrophys. J. Suppl.*, *101*, 309–334, doi:10.1086/192242.

Fligge, M., and S. K. Solanki (1997), Inter-cycle variations of solar irradiance: Sunspot areas as a pointer, *Sol. Phys.*, *173*, 427–439.

Foster, S. S. (2004), Reconstruction of solar irradiance variations, for use in studies of global climate change: Application of recent SoHO observations with historic data from the Greenwich observations, Ph.D. thesis, 430 pp., Univ. of Southampton, Southampton, U. K.

Foukal, P. (1981), Sunspots and changes in the global output of the sun, in *The Physics of Sunspots*, edited by L. E. Cram and J. H. Thomas, pp. 391–423, Sacramento Peak Obs., Sunspot, N. M.

Foukal, P. (1996), The behavior of solar magnetic plages measured from Mt. Wilson observations between 1915–1984, *Geophys. Res. Lett.*, *23*, 2169–2172, doi:10.1029/96GL01356.

Foukal, P. (1998), Extension of the F10.7 index to 1905 using Mt. Wilson Ca K spectroheliograms, *Geophys. Res. Lett.*, *25*, 2909–2912, doi:10.1029/98GL02057.

Foukal, P. (2002), A comparison of variable solar total and ultraviolet irradiance outputs in the 20th century, *Geophys. Res. Lett.*, *29*(23), 2089, doi:10.1029/2002GL015474.

Foukal, P., C. Fröhlich, H. Spruit, and T. M. L. Wigley (2006), Variations in solar luminosity and their effect on the Earth's climate, *Nature*, *443*, 161–166, doi:10.1038/nature05072.

Fröhlich, C. (2000), Observations of irradiance variations, *Space Sci. Rev.*, *94*, 15–24.

Fröhlich, C. (2003), Solar irradiance variations, in *Solar Variability as an Input to the Earth's Environment*, edited by A. Wilson, *Eur. Space Agency Spec. Publ.*, *ESA SP-535*, 183–193.

Fröhlich, C. (2006), Solar irradiance variability since 1978, *Space Sci. Rev.*, *125*, 53–65, doi:10.1007/s11214-006-9046-5.

Fröhlich, C., J. M. Pap, and H. S. Hudson (1994), Improvement of the photometric sunspot index and changes of the disk-integrated sunspot contrast with time, *Sol. Phys.*, *152*, 111–118.

Győri, L., and T. Baranyi (2006), Comparison of SOHO and Debrecen Photoheliographic Data sunspot areas for the years 1996 and 1997, in

Proceedings of SOHO 17—10 Years of SOHO and Beyond, Giardini Naxos, Sicily, Italy, *Eur. Space Agency Spec. Publ.*, *ESA SP-617*, 130.1–130.4.

Győri, L., T. Baranyi, G. Csepura, O. Gerlei, and A. Ludmany (1998), Debrecen photoheliographic data for 1986 with image supplements, *J. Astron. Data*, *4*, 1–6.

Győri, L., T. Baranyi, G. Csepura, O. Gerlei, and A. Ludmany (2000), Debrecen photoheliographic data for 1987 with image supplements, *J. Astron. Data*, *6*, 1–6.

Győri, L., T. Baranyi, J. Muraközy, and A. Ludmany (2005), Comparison of sunspot area data determined from ground-based and space-borne observation, *Mem. Soc. Astron. Ital.*, *76*, 985–988.

Hathaway, D. H., R. M. Wilson, and E. J. Reichmann (2002), Group sunspot numbers: Sunspot cycle characteristics, *Sol. Phys.*, *211*, 357–370.

Hoyt, V. D., J. A. Eddy, and H. S. Hudson (1983), Sunspot areas and solar irradiance variations during 1980, *Astrophys. J.*, *275*, 878–888.

Hudson, H. S., S. Silva, M. Woodard, and R. C. Willson (1982), The effects of sunspots on solar irradiance, *Sol. Phys.*, *76*, 211–219.

Isobe, T., E. D. Feigelson, M. G. Akritas, and G. J. Babu (1990), Linear regression in astronomy, *Astrophys. J.*, *364*, 104–113.

Krivova, N. A., L. Balmaceda, and S. K. Solanki (2007), Reconstruction of solar total irradiance since 1700 from the surface magnetic flux, *Astron. Astrophys.*, *467*, 335–346, doi:10.1051/0004-6361:20066725.

Li, K. (1999), The shape of the sunspot cycle described by sunspot areas, *Astron. Astrophys.*, *345*, 1006–1010.

Li, K. J., J. Qiu, T. W. Su, and P. X. Gao (2005), Sunspot unit area: A new parameter to describe long-term solar variability, *Astrophys. J. Lett.*, *621*, L81–L84, doi:10.1086/428941.

Mathew, S. K, V. Martínez Pillet, S. K. Solanki, and N. A. Krivova (2007), Properties of sunspots in cycle 23. I. Dependence of brightness on sunspot size and cycle phase, *Astron. Astrophys.*, *465*, 291–304, doi:10.1051/0004-6361:20066356.

Preminger, D. G., and S. R. Walton (2005), A new model of total solar irradiance based on sunspot areas, *Geophys. Res. Lett.*, *32*, L14109, doi:10.1029/2005GL022839.

Scherrer, G., et al. (1995), The Solar Oscillations Investigation–Michelson Doppler Imager, *Sol. Phys.*, *162*, 129–188.

Sivaraman, K. R., S. S. Gupta, and R. F. Howard (1993), Measurement of Kodaikanal white-light images. I—A comparison of 35 years of Kodaikanal and Mount Wilson sunspot data, *Sol. Phys.*, *146*, 27–47.

Solanki, S. K., and M. Fligge (1998), Solar irradiance since 1874 revisited, *Geophys. Res. Lett.*, *25*, 341–344, doi:10.1029/98GL50038.

Solanki, S. K., and N. A. Krivova (2003), Can solar variability explain global warming since 1970?, *J. Geophys. Res.*, *108*(A5), 1200, doi:10.1029/2002JA009753.

Solanki, S. K., and Y. C. Unruh (1998), A model of the wavelength dependence of solar irradiance variations, *Astron. Astrophys.*, *329*, 747–753.

Solanki, S. K., and Y. C. Unruh (2004), Spot sizes on Sun-like stars, *Mon. Not. R. Astron. Sci.*, *348*, 307–315, doi:10.1111/j.1365-2966.2004.07368.x.

Unruh, Y. C., S. K. Solanki, and M. Fligge (1999), The spectral dependence of facular contrast and solar irradiance variations, *Astron. Astrophys.*, *345*, 635–642.

Vaquero, J. M., M. C. Gallego, and F. Sánchez-Bajo (2004), Reconstruction of a monthly homogeneous sunspot area series since 1832, *Sol. Phys.*, *221*, 179–189, doi:10.1023/B:SOLA.0000033360.67976.bd.

Waldmeier, M. (1961), *The Sunspot Activity in the Years 1610–1960*, Shulthess, Zurich, Switzerland.

Wang, Y.-M., J. L. Lean, and N. R. Sheeley Jr. (2005), Modeling the Sun's magnetic field and irradiance since 1713, *Astrophys. J.*, *625*, 522–538, doi:10.1086/429689.

Wenzler, T. (2005), Reconstruction of solar irradiance variations in cycles 21–23 based on surface magnetic fields, Ph.D. thesis, ETH Zurich, Zurich, Switzerland.

Wenzler, T., S. K. Solanki, N. A. Krivova, and C. Fröhlich (2006), Reconstruction of solar irradiance variations in cycles 21–23 based on surface magnetic fields, *Astron. Astrophys.*, *460*, 583–595, doi:10.1051/0004-6361:20065752.

Willson, R. C., C. H. Duncan, and J. Geist (1980), Direct measurement of solar luminosity variation, *Science*, *207*, 177–179.

Worden, J. R., O. R. White, and T. N. Woods (1998), Evolution of chromospheric structures derived from Ca II K spectroheliograms: Implications for solar ultraviolet irradiance variability, *Astrophys. J.*, *496*, 998–1014, doi:10.1086/305392.

L. A. Balmaceda, GACE, IPL, Universidad de Valencia, P.O. Box 22085, E-46071 Valencia, Spain. (laura.balmaceda@uv.es)

S. Foster, Space and Atmospheric Physics Group, Blackett Laboratory, Imperial College London, Prince Consort Road, London SW7 2BZ, UK.

N. A. Krivova and S. K. Solanki, Max-Planck-Institut für Sonnensystemforschung, Max-Planck-Strasse 2, D-37191 Katlenburg-Lindau, Germany.